ICAT 2003
December 3-5, Tokyo, Japan

Extracting Rheological Properties of Deformable Objects with Haptic Vision

Naoki Ueda, *Shin-iti Hirai, Hiromi T.Tanaka

Department of Computer Science, *Department of Robotics,
Ritsumei University, 1-1-1 Noji-higashi Kusatsu Shiga, JAPAN

Abstract

In this paper, we propose a novel approach to extracting rheological properties of deformable objects based on Haptic vision, which was proposed for vision-based automatic construction of virtual environment simulators. The method consists of two parts: 1) the "touch and see" part to cause deformation behavior by exerting a known contact force on the object using a robot hand, and then observe how the deformed shape return to the original after the contact force is removed, using a range sensor and a force-feedback sensor mounted on the robot hand, 2) the analysis and parameter extraction part from the acquired range images and force-feed back data. Experimental results using springs and wheat dough demonstrated the validity and effectiveness of the proposed approach to viscoelastic parameter extraction of rheological objects.

Key words: Haptic Vision, Deformable Object modeling, Rheology, Rheological Properties, Viscoelasticity

1. Introduction

Real-world objects exhibit rich physical interaction behaviors on contact. Such behaviors depend on how heavy and hard it is when hold, how its surface feels when touched, how it deforms on contact, and how it moves when pushed, etc. These aspects of visual and haptic behavior provide important interaction cues for manipulating and recognizing objects in virtual environments. Thus, there are growing needs for haptic exploration to estimate and extract physical object properties such as mass, friction, elasticity, viscoelasticity etc.

The modeling of deformable objects have been intensively studied since late 80's. Terzopoulous et al. have proposed a modeling method of elastic objects and plastic objects in computer graphics[1][2]. Chai et al. have proposed a modeling method of plastic objects for clay[3]. Sudo et al. have proposed a vision-based modeling method of strings/ropes using a mass-spring model[4]. However, such ideal viscoelastic objects are generally very few in the real world.

One important issue of deformable object modeling is to model objects such food and tissue as meat, dough, and organs. Such objects have both elasticity and viscosity properties and are called rheological objects.

In this paper, we propose a novel approach to extraction of rheological properties of deformable objects based on Haptic vision approach, which was proposed for vision-based automatic construction of virtual environment simulators[5][6]. Haptic vision is based on active sensing and real-time image understanding methodology, which enables objects in the virtual environment to behave, and change realistically with virtual force, and to be operated with sense of touch sensation through haptic interface devices. While recent development in scanning technique of physical object properties[8], which requires human control on expensive and sophisticated robot systems, Haptic vision have pursued automatic haptic exploration approach to extraction of both geometrical and physical properties of real-world objects[7].

We develop an automatic extraction method of three viscoelastic parameters, namely C_1, C_2 for viscosity coefficients, and K_1 for elastic coefficient, of the three-element model, which have proposed as a fundamental unit for rheological object representation[11]. The method consists of two parts: The first part is the "touch and see" part with haptic vision, to cause deformation behavior by exerting a known contact force on the object using a robot hand. The contact force and the contact point are automatically selected based on the 3D shape and pose of the object so that the deformation behavior is excited most effectively and stable. Then we observe how the deformed shape returns to the original after the contact force is removed, using a range sensor and a force-feedback sensor mounted on the robot hand. The second part is the analysis and parameter extraction part. Three parameters C_1, C_2 and K_1 are extracted by analyzing changes in the displacement, i.e., the height of the deformed object, and the magnitude of the contact force from acquired range images and force-feed back data. Experimental results using springs and wheat dough demonstrated the validity and effectiveness of the proposed approach to viscoelastic parameter extraction of rheological objects.

2. Rheological objects

2.1 Characteristic of rheological objects

Rheological objects deform in response to applied external force. Suppose that an object has a natural shape, as shown in Fig.1(a). Applying external force, the object deforms as shown in Fig.1(b). After external force is removed, rheological objects do not return to the original shape, however, the deformed shape is partially restored,

as shown in Fig.1(e). This type of deformation is called bouncing deformation. And, the remaining deformation is called residual deformation. Thus, the rheological object in Fig.1(e) has three deformation properties follows: (1)residual deformation is involved, (2)bouncing displacement is involved, (3)vibrations decrease.

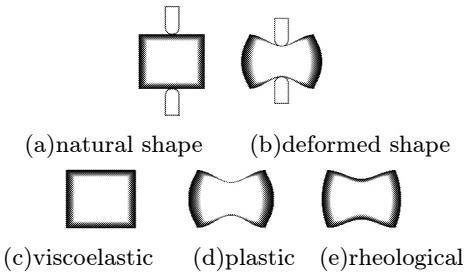

(a)natural shape (b)deformed shape

(c)viscoelastic (d)plastic (e)rheological

Fig. 1: Rheological objects

2.2 Three-element model for the rheological object representation

We adopt the three-element model proposed to describe deformation characteristic of rheological objects[11]. In the three-element model, an elastic element and a viscous element are introduced to describe the time-dependent viscous and elastic deformation of a rheological object, as shown in Fig.2(a) and Fig.2(b). The relationship between deformation and force applied can be described by either serial or parallel combinations of these two fundamental elements, and these combinations are called rheology elements.

(a)a viscous element (b)an elastic element

Fig. 2: Fundamental elements

Rheology elements do not have bouncing deformation property if the residual deformation part has only the viscous element. Rheology elements have bouncing deformation property if either the non-residual deformation part or the residual deformation part has an elastic element. And, simple harmonic motion is generated in the deformation part if an elastic element exists independently. From the above discussion, the three-element model is obtained as a rheology element which consists of minimum number of fundamental elements, as shown in Fig.3.

The three-element model is formulated as follows. Let P_{n-1} and P_n be two end points of the rheological element. Elastic and viscosity coefficients in the non-residual deformation part are denoted as K_1 and C_1 respectively. The other viscosity coefficient in the residual deformation part is denoted as C_2. The natural length of the non-residual deformation part is given by L_1, and the natural length of the residual deformation part is given by L_2. Let M be mass at each point. Let P_n^1 be the position of a connecting point between the non-residual and residual deformation parts. Furthermore, the length of the model $\mathsf{d}_n = \mathsf{P}_n - \mathsf{P}_{n-1} = L_1 + L_2$ is defined. Since these positions P_{n-1}, P_n^1 and P_n lie on a straight line, P_n^1 can be defined by a parameter k as follows: $\mathsf{P}_n^1 = k\,\mathsf{d}_n + \mathsf{P}_{n-1}$. Here, a time-varying direction vector is defined as $\mathsf{e}_n = \mathsf{d}_n / |\mathsf{d}_n|$, and also time varying length coefficient is defined as $Z_n = k|\mathsf{d}_n|$. Let F_e be force applied to a mass point P_n. The force F_e equals to force acting on the non-residual deformation part, that is,

$$F_\mathsf{e} = -C_1 \dot{Z}_n \mathsf{e}_n - K_1 (Z_n - L_1)\mathsf{e}_n. \quad (1)$$

Also, the force F_e coincides with the force caused by the damper of the residual deformation part, that is,

$$F_\mathsf{e} = -C_2 \left(\frac{\mathrm{d}}{\mathrm{d}t}(|\mathsf{d}_n| - Z_n)\right)\mathsf{e}_n. \quad (2)$$

Here, the force applied to a mass point P_n is defined as F_a. Consequently, the dynamic equation of the mass point P_n is denoted as,

$$M\ddot{\mathsf{P}}_n = F_\mathsf{e} + F_\mathsf{a}. \quad (3)$$

From three equations (1), (2) and (3), we can compute the deformation of a rheological object.

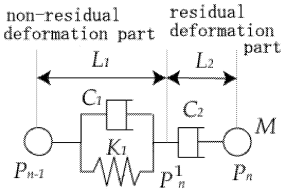

Fig. 3: Three-element model

3. Rheological object modeling with haptic vision

In this study, viscoelastic parameters of a rheological object are extracted based on Haptic vision approach, as shown in Fig.4. In step 1, we actively observe an object in the scene from multiple viewpoints using a haptic vision sensor, consisting of a range sensor and a CCD camera, to acquire 3D shape, posture and the center of gravity. In step 2, based on the acquired 3D geometrical properties, a contact point and the direction of contact force are selected and exerted on the object to cause deformation behavior most effectively and stable. We call this dynamic scene of object's response as a pilot event where a prototypical behavior due to the objective physical property is exhibited on response to a known contact force. In step 3, the deformation behavior is observed using haptic vision sensor and a force-feed back mounted on the robot. In step 4, the viscoelastic properties of the object are then estimated and extracted through motion analysis from acquired range image and force-feed back data.

3.1 Selecting a contact point and contact force

Our approach to rheological property estimation by "Push" operation by a robot hand is as follows. We assume that a rheological object is placed on a horizontal support plane at a stable pose. Since the support plane is horizontal, we have to exert contact force on the center of gravity of the object, perpendicular to the support plane,

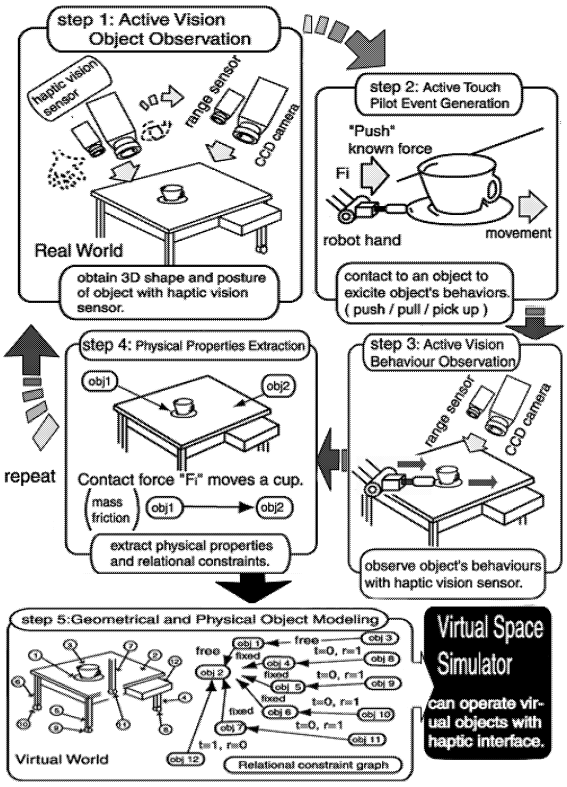

Fig. 4: Haptic Vision Approach

so that it does not make it move nor rotate. Therefore, a contact point is chosen at the intersection of the object surface with a perpendicular line passing through the 2D mass center of the object in the top view.

3.2 Active observation of deforamation behavior

A Contact point, contact force and a viewpoint for observing deformation behavior of an object are shown in Fig.5.

Step 1. We observe the object from the top view point, and estimate the 2D mass center G_{top} and a line of symmetry L of the object in the top view image as shown in Fig.5(a). Then, we estimate the perpendicular plane of symmetry S including L and the center of gravity as shown in Fig.5(b).

Step 2. The haptic vision sensor with a range finder is placed at the viewpoint (VO in Fig.5(b)) perpendicular to S in order to observe the deformation behavior caused by downward "Push" operation, by a robotic hand.

Step 3. Contact force F is exerted downword by Push operation on the contact point P_{c} at the intersection of the object surface and a line perpendicular to the support plane that goes through the 2D mass center G_{top}.

Step 4. The 3D deformation behavior of the object is observed using CCD camera and a range finder. The transition of contact force F is simultaneously observed using a force feed-back sensor mounted on the robot hand.

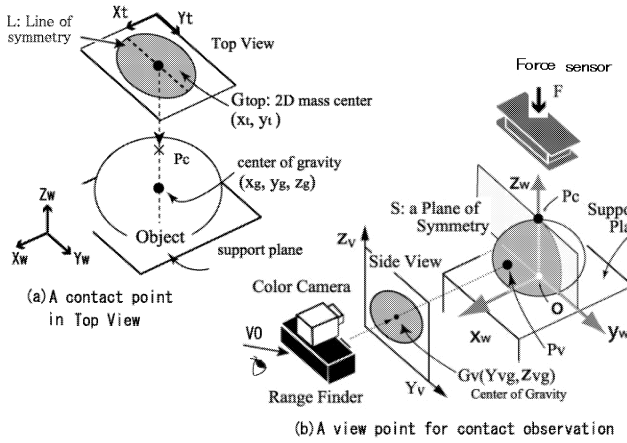

Fig. 5: A contact point, contact force and a view point

3.3 Extracting viscoelastic parameters of rheological objects

Fig.6 shows the prototypical deformation behavior of a rheological object under pressure and after pressure is released, namely transition of contact force and displacement height of the object. The deformation process is divided into three phases at time T_{c} of contact, at time T_{s} of the maximum displacement height reached and at time T_{e} of the contact force released. Then, viscoelastic parameters of the three-element model, C_1, C_2 and K_1, are estimated step by step fashion at each phase, as shown in Fig.6(a), (b), (c) and (d)

Phase 1 ($T_{\mathrm{c}} \leqq T < T_{\mathrm{s}}$): Both residual and bouncing non-residual deformation parts of the objects deform by contact force F, as shown in Fig.6

Phase 2 ($T_{\mathrm{s}} \leqq T < T_{\mathrm{e}}$): When displacement height H of the object is reached at the specified value, the robot stops "Push" operation so that the displacement height is kept constant, while the pressure measured as contact force gradually decreases and converges to the constant value F_∞ at T_{e}. This attenuation behavior of the contact force F_∞ depends on the values of the viscous coefficients C_1 and C_2, and the elastic coefficient K_1, and the convergence value of the contact force depends on K_1.

Phase 3($T_{\mathrm{e}} \leqq T$): After the external force is released at T_{e}, pressure i.e., the size of the contact force soon become zero. Since the bouncing deformation part of the object returns to the original while the residual deformation part remain deformed, the displacement height of the object gradually decreases and converges to the constant value H_∞. This attenuation behavior of the displacement height H depends only on C_1 and K_1.

In the above phases, C_1, C_2 and K_1 of the three-element model are estimated as step-by-step fashion as follows.

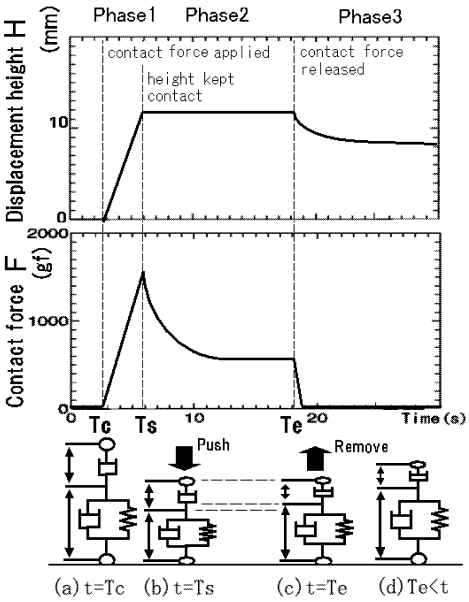

Fig. 6: Transition of contact force F and displacement height

Step1:Acquire the relation of C_1, C_2 and K_1 from the attenuation curve of the contact force in Phase2

The relation among C_1, C_2 and K_1 is obtained from the attenuation of the contact force F in Phase 2 in Fig.6. The attenuation behavior of the contact force F in Phase 2 is approximated by the following exponential function,

$$F = F_0 e^{\frac{-t}{\tau}} + F_\infty \tag{4}$$

where F_0 is the difference of the contact force at T_s and at T_∞, F_∞ is the convergence value of the force at T_∞. Here, τ is called the relaxation time, and is denoted as,

$$\tau = \frac{\eta}{G} \tag{5}$$

where η is a viscosity coefficient and G is an elastic coefficient. In Phase2, since the attenuation of F depends on C_1, C_2 and K_1 the relaxation time τ has to be described by three-element parameters C_1, C_2 and K_1.

First, time varying length coefficient Z_n is acquired by removing F_e from eq.(1) and eq.(2). The length of the model d_n is a constant, since displacement height H is kept constant in Phase 2. Thus, it is obtained as $\mathrm{d}/\mathrm{d}t|d_n| = 0$. Then, $\dot{Z}_n$ is denoted as,

$$\dot{Z}_n = -\frac{K_1}{C_1 + C_2} Z_n + \frac{K_1 L_1}{C_1 + C_2}. \tag{6}$$

Here, $\dot{Z}_n$ can be defined in the following differential equation with integration constant a as follows:

$$\dot{Z}_n = -\frac{K_1 a}{C_1 + C_2} e^{-\frac{K_1 a}{C_1 + C_2}}. \tag{7}$$

Next, by substituting eq.(2) with eq.(7), the attenuation curve of the contact force F is denoted as,

$$F = \frac{a K_1 C_2}{C_1 + C_2} \cdot e^{\frac{-K_1 t}{C_1 + C_2}}. \tag{8}$$

Here, by comparing eq.(4) with the exponent of eq.(8), the relaxation time τ is described with C_1, C_2 and K_1 as follows:

$$\tau = \frac{C_1 + C_2}{K_1}. \tag{9}$$

Therefore, the relation among τ and three-element parameters C_1 and C_2 and K_1 is obtained.

Step2: Acquire the relation of C_1 and K_1 from the attenuation of the displacement height H in Phase3

Similarly, the relation between C_1 and K_1 is obtained from the attenuation of the displacement height H in Phase 3 in Fig.6. The displacement height H is also approximated by the following exponential function,

$$H = H_0 e^{\frac{-t}{\gamma}} + H_\infty \tag{10}$$

where H_0 is the bouncing deformation i.e., the difference between the displacement height H at T_e and at T_∞, H_∞ is the convergence value of the contact force at T_∞. Here, γ is called a delay time, and it depends on the viscosity coefficient η and the elastic coefficient G. The delay time γ is denoted as,

$$\gamma = \frac{\eta}{G}. \tag{11}$$

Therefore, the delay time γ can be estimated by fitting eq.(10) to measured values of the displacement height curve in Phase3, and the relation of C_1 and K_1 is obtained as follows:

$$\gamma = \frac{C_1}{K_1}. \tag{12}$$

Step3: Estimate the elastic coefficient K_1

Hooke's law is applied to the convergence value of the contact force F_∞ in Phase 2 and the bouncing deformation H_0 in Phase 3 in Fig.6, because the bouncing deformation depends on an elastic element. Convergence value F_∞ of the contact force can be estimated from eq.(4), and the bouncing deformation H_0 can be estimated from eq.(10). Finally, the elastic coefficient K_1 can be estimated from eq.(13) by using Hooke's law.

$$F_\infty = K_1 H_\infty. \tag{13}$$

Step4:Estimate the viscocity coefficients C_1 and C_2

C_1 is determined from K_1 and eq.(12). Finally, C_2 is determined from C_1, K_1 and eq.(9).

4. Experiment

Viscoelastic parameters of rheological objects are extracted by the proposed method using haptic vision system, as shown in Fig.7. Haptic Vision system consists of two robot hands called vision and haptic robots where both a CCD camera and a range sensor is mounted on the vision robot, and a load-cell unit is mounted on the haptic robot.

Wheat Dough of size $85mm * 60mm * 40mm$ made of flour and water as 3:1 was used as a rheological object through our experiments.

First, the accuracy of our system is evaluated by estimating elastic coefficients of three kinds of springs with known elastic coefficients. Fig.8 shows the transition of contact force and displacement height of spring objects. All three elastic coefficients were estimated within 5% error, as shown in Table.1.

Table 1: Estimation results of elastic coefficients of spring objects

	estimated(kgf/mm)	true(kgf/mm)	error(%)
spring1	0.386	0.37	4.26
spring2	0.729	0.76	4.12
spring3	1.175	1.13	3.97

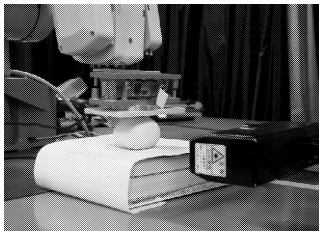

Fig. 7: Haptic vision system

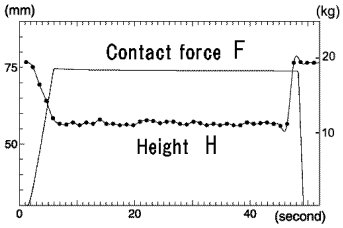

Fig. 8: Transition of contact force F and displacement height of spring objects

4.1 Estimation of viscoelastic parameters of rheological object

Four kinds of experiments on estimation of viscoelastic coefficients for wheat dough were done, each for two kinds of pushing speeds, SP0(about 1.3mm/sec) and SP2(about 7.7mm/sec) and each for two kinds of displacement height, 10mm and 15mm. Fig.9(a) and Fig.9(b) show the transition of contact force and displacement height with SP0 and SP2, respectively. We fitted eq.(4) to the attenuation of contact force in Phase2 and fitted eq.(10) to the attenuation of displacement height in Phase3. We then obtained the values of τ, γ, H_0 and F_∞ from the above fitting results, to estimate C_1, C_2 and K_1 using eq.(9), eq.(12) and eq.(13).

Fig.10 shows the results of curve fitting of eq.(4) in Phase2 with SP0, where the measured values of the force F attenuation were shown in the solid curve and the fitted curve of eq.(4) was shown in the dotted curve. Parameters were estimated as $F_0 = 9.26 * 10^2$gf, relaxation time $\tau =$ 38.3sec and the convergence value of the force $F_\infty = 5.01 * 10^2$gf with the displacement height=10mm.

Similarly, Fig.11 shows the results of curve fitting of eq.(10), where the measured values of the displacement attenuation was shown in the dotted curve and the fitted curve of eq.(10) was shown in the solid line. These parameters were estimated as the bouncing deformation $H_0 =$ 0.98mm, delay time $\gamma =$ 16.8sec and permanent strain $H_\infty = 7.44$mm at an amount of displacement height=10mm. Table.2 shows the results of curve fitting of eq.(4) and eq.(10) for rheological parameter extraction: relaxation time τ, convergence value F_∞, delay time γ and bouncing deformation H_0.

Table.3 shows the estimation results of viscoelastic parameters C_1, C_2 and K_1 of the three-element model of wheat dough. When the deformation parameters are estimated from real objects, it is regarded that the values estimated are valid as long as the order of the value estimated is consistent, because the value estimated changes greatly against too small changes in temperature and humidity, etc. Therefore, we consider that the estimated value of C_1, C_2 and K_1 are valid except for the case with SP2-15mm, as shown in tables.3.

The main reason for that inconsistency is nonlinearity of viscoelastic coefficients to contact force. The magnitude of displacement height must be proportional to contact force, if elastic coefficient has linearity, and contact force is also proportional to "Push" speed if the viscosity coefficient has linearity. However, viscoelastic property seem to have nonlinearity when the size of displacement and "Push" speed are large, while it show linearity when the size of displacement and "Push" speed is small.

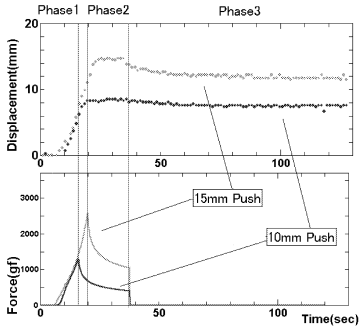

(a)SP0(1.3mm/sec)

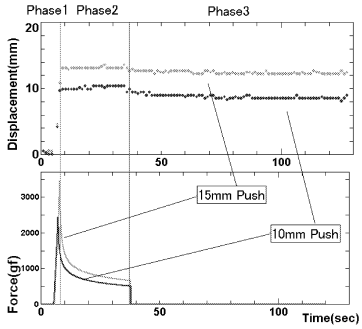

(b)SP2(7.7mm/sec)

Fig. 9: Transition of contact force and displacement height of wheat dough

4.2 Evaluation using three-element simulation model

Next, we evaluate the accuracy of the estimated values of C_1, C_2 and K_1 using the three-element simulation model [12], where C_1, C_2 and K_1 were used as input to simulate deformation of a rheological object. Then, we compared the result of deformed shape from simulation with real with simulated shape of the object. Fig.12 show the comparison of real range image with an image of simulated shape of dough after the displacement height converges. The values of both bouncing deforma-

tion and residual deformation were computed displacement as height from simulation result of deformed shape. Table.4 shows these comparison results. These experimental results demonstrated that the validity of the proposed approach, and the effectiveness of the three-element model for modeling viscoelastic properties of rheological objects.

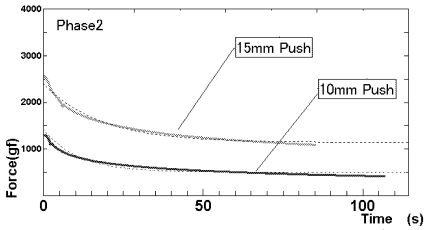

SP0, 10mm: $F = 9.26 * 10^2 \cdot e^{\frac{-t}{38.3}} + 5.01 * 10^2$

SP0, 15mm: $F = 12.7 * 10^2 \cdot e^{\frac{-t}{62.7}} + 11.4 * 10^2$

Fig. 10: τ estimation from contact force attenuation with SP0

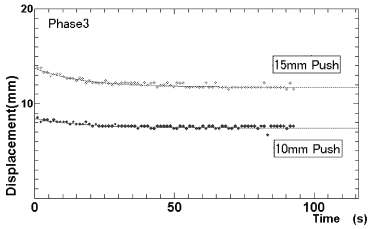

SP0, 10mm: $H = 0.98 \cdot e^{\frac{-t}{16.8}} + 7.44$

SP0, 15mm: $H = 2.01 \cdot e^{\frac{-t}{17.2}} + 11.7$

Fig. 11: γ estimation from displacement height attenuation with SP0

Table 2: Estimation results of fitting attenuation curves of contact force and displacement height of eq.(4) and eq.(10)

"Push" speed (mm/sec)	displacement height (mm)	τ (sec)	F_∞ (10^2gf)	γ (sec)	H_0 (mm)
1.3 (SP0)	10	38.3	5.01	16.8	0.98
	15	62.7	11.4	17.2	2.01
7.7 (SP2)	10	37.4	6.42	17.6	1.27
	15	36.9	8.26	21.4	0.63

5. Conclusion

We have proposed a novel approach to extraction of rheological properties of deformable objects based on haptic vision approach. First, we exert a known contact force on a rheological object using a robot hand to cause deformation behavior. Then we observe how the deformed shape return to the original after the contact force is removed, using a range sensor and a force-feedback sensor mounted on the robot hand. From the analysis of acquired force data and range image, three viscoelastic parameters C_1, C_2 and K_1 of the three-element model for the rheological object representation were obtained as step by step fashion.

The effectiveness and validity of the proposed method were demonstrated through the experimental results.

Table 3: Estimation results of viscoelastic coefficients

"Push" speed (mm/sec)	displacement height (mm)	C_1 (kgf · s/mm)	C_2 (kgf · s/mm)	K_1 (kgf/mm)
1.3 (SP0)	10	8.59	11.0	0.511
	15	9.73	26.0	0.565
7.7 (SP2)	10	8.95	10.0	0.507
	15	27.9	20.3	1.30

Table 4: Comparison of real v.s. simulated values

"Push" speed (mm/sec)	displacement height (mm)	bouncing deformation(mm)		residual deformation(mm)	
		real	simulated	real	simulated
1.3 (SP0)	10	2.15	2.94	7.85	7.06
	15	2.86	7.90	11.7	7.10
7.7 (SP2)	10	1.58	2.20	8.42	7.80
	15	1.98	1.77	13.0	13.2

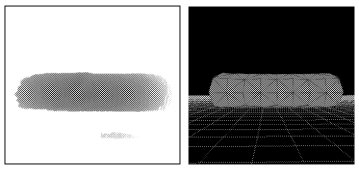

(a)real range image (b)simulated image

Fig. 12: Real v.s. simulated shape

References

1. D. Terzopoulous, J. Platt, A. Barr, and K. Fleisher: "Elastically Deformable Models," Computer Graphics, Vol.21, No.4, pp.205-214 (1987).
2. D. Terzopoulous and K. Fleisher: "Modeling Inelastic Deformation," Computer Graphics, Vol.22, No.4, pp.269-278 (1988).
3. Y. Chai and G.R. Luecke: "Virtual Clay Modeling Using the ISU Exoskeleton," Proc. IEEE Virtual Reality Annual International Symposium, pp.76-80 (1988).
4. Katsuhito Sudoh, Koh Kakusho and Michihiko Minoh: "Modeling a String from Observing the Real Object," International Conference on Virtual System and MultiMedia (VSMM) (2000).
5. Hiromi T. Tanaka, and Kiyotaka Kushihama: "Haptic Vision: Vision-Based Haptic Exploration," Proc. IEEE 16th International Conference on Pattern Recognition, Vol.2, Session1.7 Robotics, Vol.II, pp.852-855 (2002)
6. Hiromi T. Tanaka, N. Ueda, K. Kushihama and S. Hirai: "Vision-based Haptic Exploration," Proc. IEEE Int. Conf. on Robotics and Automation(ICRA2003) (2003).
7. Hiromi Tanaka and Kayoko Yamasaki: "Extracting Relational Constraints among Objects with Haptic Vision for Haptic-Interfaced object Manipulation," Proc. the 12th ICAT (2002).
8. D.K. Pai, K. van den Doel, D.L. James, J. Lang, J. E. Lloyd, J.L. Richmond and S.H. Yau: "Scanning Physical Interaction behavior of 3D objects," in Computer Graphics(ACM SIGGRAH 2001 conference Proceedings) (2001).
9. Kengo Nishimura and Hiromi T.Tanaka: "Active Shape Inferring Based on the Symmetry in Stable Poses-Shape from Function Approach-," IEEF Proc.of International Conference on Pattern Recognition'96(13thICPR), pp136-140 (1996).
10. D.D. Milasinovic: "Rheological-dynamical analogy: Modeling of fatigue behavior," Int J Solids Struct, Vol.40, No.1, pp.181-217 (2003).
11. Shinichi Tokumoto, Shinichi Hirai and Hiromi Tanaka: "Constructing Virtual Rheological Objects," Proc. World Multiconference on Systemics, Cybernetics and Infomatics, pp.106-111 (2001).
12. Masafumi Kimura, Yuuta Sugiyama, Seiji Tomokuni, and Shinichi Hirai: "Constructing Rheologically Deformable Virtual Objects," Proc. IEEE Int. Conf. on Robotics and Automation (2003).